

Develop a sustainable wet shotcrete for tunnel lining using industrial waste: a field experiment and simulation approach

Jinkun Sun^{*1,2}, Rita Yi Man Li³, Lindong Li¹, Chenxi Deng⁴, Shuangshi Ma⁴ and Liyun Zeng¹

¹ Civil and Architectural Engineering Institute, Panzhihua University, Panzhihua 617000, China

² Rattanakosin International College of Creative Entrepreneurship, Rajamangala University of Technology Rattanakosin, Bangkok 10700, Thailand

³ Sustainable Real Estate Research Center, Hong Kong Shue Yan University, Hong Kong, 999077, China

⁴ School of Civil Engineering and Environment, Xihua University, Chengdu 610039, China

(Received April 2, 2022, Revised May 16, 2023, Accepted May 25, 2023)

Abstract. Fast infrastructure development boosts the demand for shotcrete. Despite sand and stone being the most common coarse and fine aggregates for shotcrete, excessive exploration of these materials challenges the ecological environment. This study utilized an industrial solid waste, high-titanium heavy slag, blended with steel fibers to form Wet Shotcrete of Steel Fiber-reinforced High-Titanium Heavy Slag (WSSFHTHS). It investigated its workability, shotcrete performance and mechanical properties under different water-to-cement ratios, fly ash content, superplasticizer dosage, and steel fiber content. The tunnel excavation and support were investigated by conducting finite element numerical simulation analysis and was used in 3 tunnel lining pipes in Zhonggouwan tailing pond. The major findings are as follows: (1) The water-to-cement ratio (w/c ratio) significantly impacted the compressive strength of WSSFHTHS. The highest 28-day compressive strength of 60 MPa was achieved when the w/c ratio was 0.38; (2) Adding fly ash improved the workability and shotcrete performance and strength development of WSSFHTHS. The best anti-permeability performance was achieved when the fly ash constituted 15%, with the lowest permeability coefficient of 4.596×10^{-11} cm/s; (3) The optimum superplasticizer dosage for WSSFHTHS is 0.8%. It provided the best workability and shotcrete performance. Excessive dosage resulted in water bleeding and poor aggregate encapsulation, while insufficient dosage decreased flowability and adversely affected shotcrete performance; (4) The dosage of steel fibers significantly impacted the flexural and tensile strength of WSSFHTHS. When the steel fiber dosage was 45 kg/m³, the 28-day flexural and tensile strengths were 8.95 MPa and 6.15 MPa, respectively; (5) By integrating existing shotcrete techniques, the optimal lining thickness was 80 mm for WSSFHTHS per simulation. The results revealed that after using WSSFHTHS, the displacement of the tunnel surrounding the rock significantly improved, with no cracks or hollows, similar to the simulation results.

Keywords: construction materials; fly ash; high titanium heavy slag; safety; shotcrete; simulation; steel fibre; sustainability

1. Introduction

Shotcrete requires no vibration or compaction and involves spraying the mix at a high velocity onto the receiving surface. Through repeated and continuous impact, the mixture is compacted and densified. It can be applied in any direction using delivery hoses, allowing fast construction. Owing to the abovementioned characteristics, shotcrete is widely utilized in initial tunnel support (Li 2021, Sakoparnig *et al.* 2023). Rapid infrastructure development like railways, superhighways and bridges increases the demand for shotcrete. However, sand and stone are the most common coarse and fine aggregates for shotcrete. Excessive exploration of these materials challenges the ecological environment. The Chinese government currently encourages using industrial solid waste to realize green development (Sun *et al.* 2023). For

example, the Ministry of Industry and Information Technology and the Ministry of Housing and Urban-rural Development jointly issued the Action Plan for Promoting the Production and Utilization of Green Building Materials.

High titanium heavy slag is one of the industrial solid waste in Panzhihua and Xichang. It is the titaniferous slag formed in the blast-furnace smelting of vanadium Titanomagnetite after natural cooling. The titanium dioxide (TiO₂) content is as high as 20% ~ 24%. At present, it is hard to extract titanium from such slag. As a result, it cannot be effectively used. Huge slag piles are formed in long-term accumulation, which challenges the sustainable use of resources (Huang 2006). Zhen *et al.* (2021) use high titanium heavy slag as the natural pre-wetting material in concrete with better two-point strength.

If an appropriate amount of steel fibre is added to concrete and the steel fibre is spread homogeneously in the carrier, a new type of multiphase composite material can be made, namely, steel fibre-enhanced concrete (Liu 2020). Steel fibers are widely used as a reinforcement material to improve the mechanical properties of concrete, such as strength, ductility, and toughness (Guler and Akbulut 2022).

*Corresponding author, Ph.D., Professor,
E-mail: paxf66290838@163.com

After adding the steel fibre, the concrete performance is greatly improved. The steel fibre in concrete plays a vital role in bridging. It can change the load transfer by suppressing the development of cracks inside the carrier under external loads and preventing the formation and expansion of macro cracks, thereby improving the concrete tensile strength, shear resistance and bending strength determined by the principal tensile stress (He 2013).

At present, tunnel engineering has various potential hazards. Common problems include lining deformation, lining cracks, and tunnel water leakage (Dai *et al.* 2020). These problems are associated with tunnel safety and quality and threaten tunnel durability, leading to the early retirement of the tunnel. Xue *et al.* (2014) analyzed the deformation and instability mechanism characteristics of surrounding rock and support structure using a geological engineering survey, theoretical analysis and field monitoring, which is of reference significance for tunnel safety prevention in similar projects. Pisova and Hilar (2017) studied the application of sprayed waterproof membrane tunnel lining in hard rock and soft ground tunnel construction and proposed building a safe waterproof tunnel lining. It improves concrete materials by reducing potential tunnel damages and optimizes the strength and flexibility of tunnels to improve the structural durability of lining, thereby enhancing the safety of tunnels during their life cycles. It reduces maintenance costs and promotes environmentally friendly infrastructure (Liu 2019). There are few studies on preparing shotcrete for tunnel lining by adding steel fibres with industrial solid wastes as coarse and fine aggregate, and the shotcrete used in many projects cannot meet the strength requirements and quickly forms cracks, leading to poor flexibility, durability (Mou 2014, Yang 2015) and tunnel safety in turn.

The construction processes for shotcrete can be classified into dry and mix shotcrete. Shotcrete originated from the development of machine-applied mortar and has a history of over a hundred years. Dry shotcrete was the earliest construction technique employed for tunnel support. It involves pre-mixing coarse and fine aggregates, cementitious materials, and powdered accelerators in specific proportions. Using a dry shotcrete machine and compressed air supplied by an air compressor, the dry mixture and pressurized water are thoroughly mixed and then sprayed onto the receiving surface through a delivery pipe at the nozzle. Due to the water requirement in dry shotcrete being controlled by the shotcrete operator, it heavily relies on their experience, resulting in poorer accuracy in water-to-cement ratio control, significantly affecting the shotcrete performance (Hemphill 2013, Thomas 2009).

To address a series of issues such as poor quality, high rebound rate, and excessive dust generation associated with dry shotcrete, the wet shotcrete technique was developed. The process involves pre-mixing coarse aggregates, fine aggregates, cementitious materials, and water according to the designed mix proportion to create wet-mix concrete. Once the mixture reaches an inevitable slump and flowability, it is pressure-fed to the nozzle through a wet shotcrete machine, either pumping or air delivery. At the

nozzle, liquid accelerators are mixed with the wet mixture and then sprayed onto the receiving surface. The main difference between wet shotcrete and dry shotcrete is applying water at the nozzle. In dry shotcrete, water is added at the nozzle to mix with the dry material before spraying onto the receiving surface, while in wet shotcrete, liquid accelerators are added at the nozzle and water is pre-mixed with the materials to create wet concrete (Duarte *et al.* 2019).

Regarding WSSFHTHS, it is necessary to integrate existing shotcrete techniques and compare them with conventional wet shotcrete. Under the optimal mix proportion conditions, experiments on shotcrete rebound and thickness are conducted on WSSFHTHS to determine the optimal spraying distance and air pressure, thereby optimizing the construction process. It replaced high titanium heavy slag with natural sand and stone as the coarse and fine aggregate of shotcrete to mix with steel fibre to form WSSFHTHS. A study was conducted on the basic performance of this new type of lining concrete. WSSFHTHS was used in 3 tunnel-lining pipes in Zhonggouwan tailing pond. Ansys finite element analysis software is used for a simulation analysis to study lining safety. The research results improve the utilization rate of high titanium heavy slag and the safe use of WSSFHTHS in tunnel engineering.

By integrating existing shotcrete techniques, comparing them with conventional wet shotcrete, and conducting experiments on shotcrete rebound and thickness under optimal mix proportion conditions, the aim is to determine the optimal spraying distance, and air pressure and optimize the construction process for SFHSWS.

2. Raw materials and mix ratio design of WSSFHTHS experiments

2.1 Experimental materials and preparation of test pieces

2.1.1 WSSFHTHS production

The gravel and sand containing high titanium heavy slag produced by some companies were selected as the main coarse and fine aggregates of WSSFHTHS. The cement was the P.O42.5R ordinary Portland cement, produced by production industries at Panzhihua City in China. The silica fume is the grade I silica fume was produced by some science and technology Companies at Chengdu City in China. The fly ash was the grade I fly ash produced by some relative filtering media companies. The water-reducing agent is Q8081 balanced type liquid polycarboxylic acid high-performance water-reducing agent produced by some building materials company in Shaanxi Province. The accelerator used was a liquid alkali-free accelerator. Some rubber production industries produced steel fibre in Hebei Province.

2.1.2 Preparation of test pieces

The concrete slab spray was used for preparing the test pieces. WSSFHTHS was sprayed on a mould of 450 ×

Table 1 Level influencing factors

Horizontal variable	Influence factor			
	A: Water binder ratio	B: Fly ash (%)	C: Water reducing agent (%)	D: Steel fibre (kg/m ³)
1	0.34	0	0.6	35
2	0.36	10	0.8	40
3	0.38	20	1.0	45
4	0.40	30	1.2	50

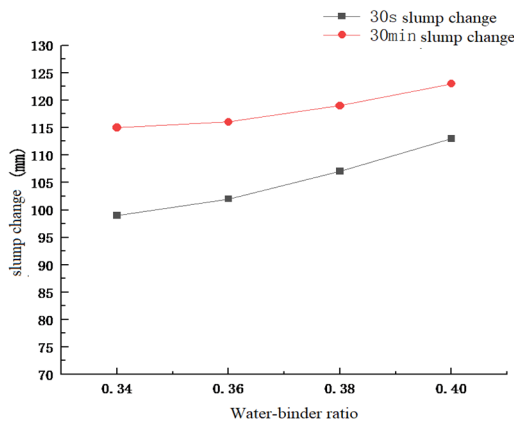


Fig. 1 Slump changes with water-binder ratio and time

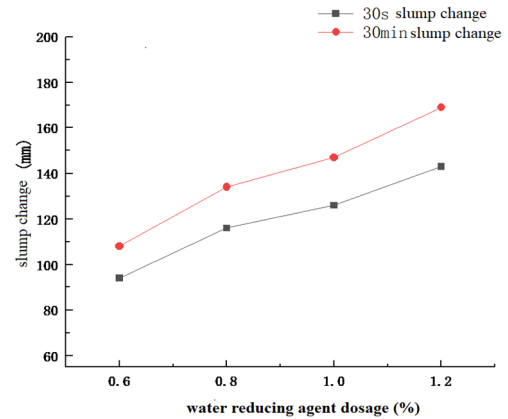


Fig. 3 Slump change with water reducing agent dosage and time

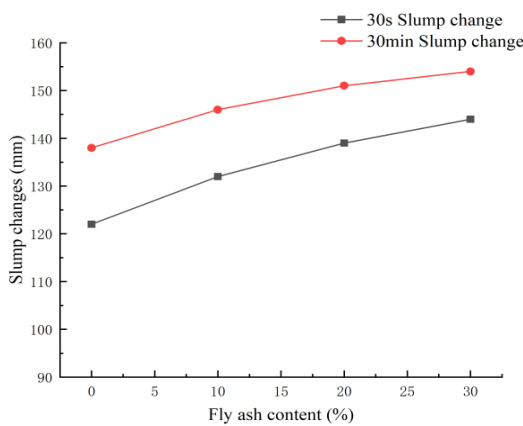


Fig. 2 Slump changes with fly ash content and time

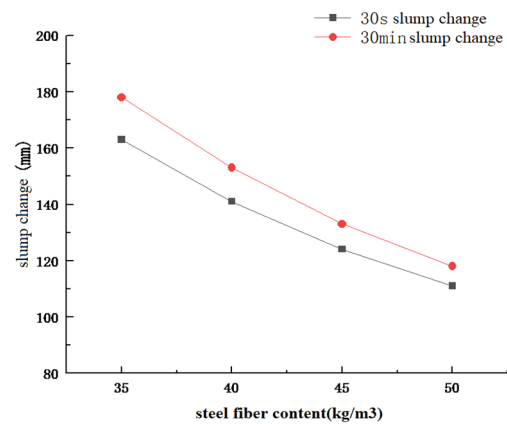


Fig. 4 Slump change with steel fibre content and time

450 × 150 mm . The mould was covered with a film, maintained for 1 d after spray, and then removed. Then, the test piece was transferred to a standard curing room (20 ± 2°C with humidity ≥ 95% for 7 days. The slab test piece was cut into a 100 × 100 × 100 mm cube with a cutter for testing the compressive strength, a 100 × 100 × 100 mm test piece for testing the folding strength, and a 150 × 150 × 150 mm test block for testing the splitting tensile strength.

2.2 Test mix ratio design

Different water-binder ratios, mineral admixture contents, additive contents, and steel fibre contents affect the performance of shotcrete. Thus, the orthogonal test

method was adopted, with water-binder ratio, fly ash content, water-reducing agent dosage and steel fibre content as the four main constituents for the WSSFHTHS. We then adopted different mix ratios by changing the level factors. The optimum mix ratio was computed through the orthogonal test (Shuyuan 2016). Four level influencing factors were adopted in the trial. The variable level of each element is shown in Table 1. The L16 (44) orthogonal test table was adopted for the calculation.

2.3 Analysis of orthogonal test result

2.3.1 Working performance analysis

The impacts of different water-binder ratios, fly ash contents, water reducing agent dosage and steel fibre

contents on the working performance of WSSFHTHS (slump, cohesiveness, water retention property) are shown in Figs. 1-4. The slump test was done according to GB/T 50080 for Test Method of Performance on Ordinary Fresh Concrete. The slump cone conformed with the industrial standard JG/T 248 Apparatus for Concrete Slump Test. The time spent on the lift-off of the slump cone should be controlled at 3 S~7 S.

The results showed that the slump of WSSFHTHS increased as the water-binder ratio increased (Liu 2015). When the water-binder ratio was 0.34, the 30 s slump of the mixture was 99 mm. When the water-binder ratio was 0.36, the 30 s slump of the mixture was 102 mm, which increased by 3.03%. When the water-binder ratio was 0.38, the 30 s slump of the mix was 107 mm, increased by 8.08%. When the water-binder ratio was 0.40, the 30 s slump of the mixture was 113, increased by 14.14%.

As the proportion of fly ash in cementing materials increased, the slump value of WSSFHTHS also increased (Li 2012). When the fly ash content was 0%, the 30 s slump of the mixture was 122 mm. When the fly ash content was 30%, the slump was 144 mm, increasing by 18.03%. The 30 min slump change added fly ash reduced the loss rate of the slump. Fly ash plays the role of plasticization on

WSSFHTHS. Meanwhile, the test also showed that as the fly ash content increased, the mixture's water retention property and cohesiveness could be improved.

After adding the polycarboxylic acid high-efficiency water-reducing agent, the slump of WSSFHTHS increased (Ding *et al.* 2019). When the water-reducing agent dosage was 0.6%, the 30 s initial slump of the mixture was 94 mm. When the mixing amount was 1.2%, the initial slump was 143 mm, increasing by 52.13%. The test result showed that although the water-reducing agent increased the mixture liquidity, the slump value of the mixture significantly reduced as time increased.

The slump of WSSFHTHS gradually decreased as the steel fibre content increased (Zhang and Pan 2021). When the steel fibre content was 35 kg/m³, the initial slump of the mixture was 141 mm, which was reduced by 13.50% compared with that of the reference mixture. When it was 50 kg/m³, the slump was 96 mm, reduced by 41.10%. Adding steel fibre could increase the slump prevention ability of shotcreting, and the slump loss gradually decreases as time goes on. Nevertheless, when the steel fibre content exceeded 45 kg/m³, the cohesiveness of WSSFHTHS mixture began to decline.

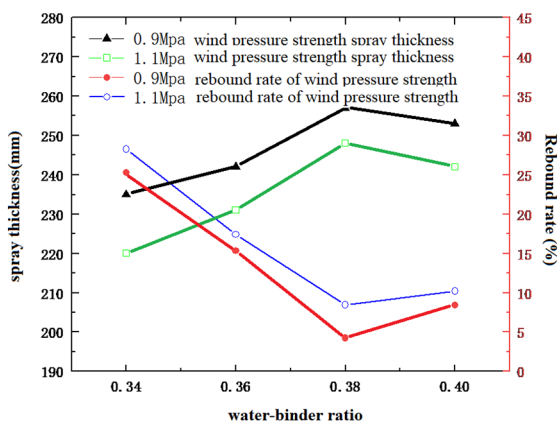


Fig. 5 The influence of different water-binder ratios and wind pressure on spray thickness and rebound

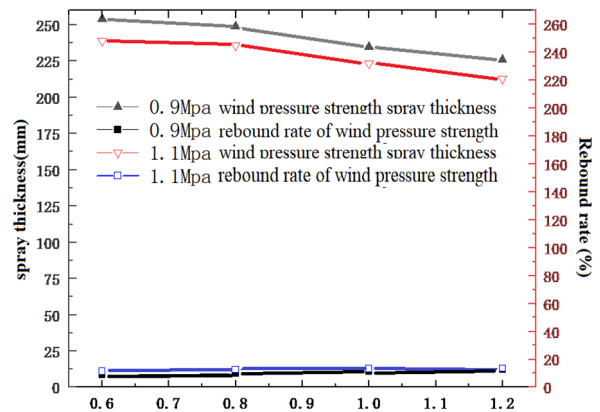


Fig. 7 The impact of different water-reducing agent content and wind pressure on spray thickness and rebound

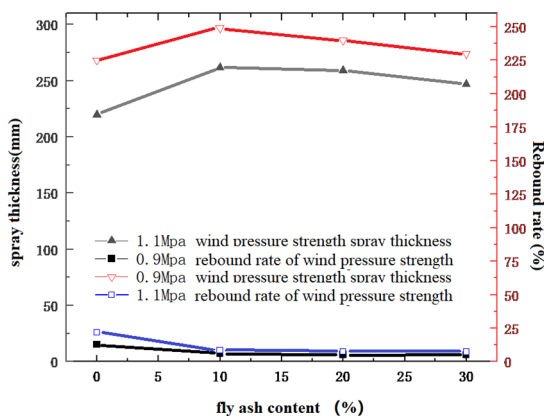


Fig. 6 The influence of different fly ash content and wind pressure on injection thickness and rebound

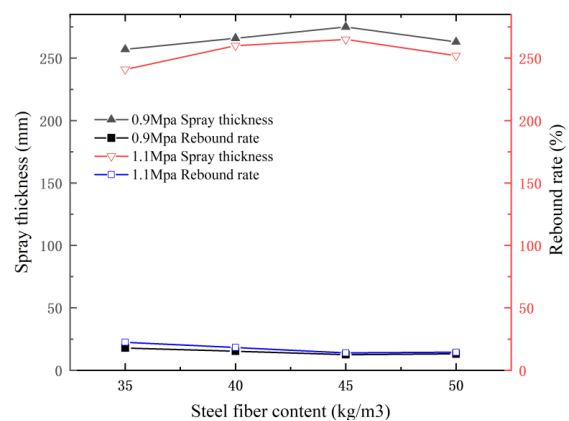


Fig. 8 The influence of different water-reducing agent content and wind pressure on spray thickness and rebound

2.3.2 Shotcrete performance analysis

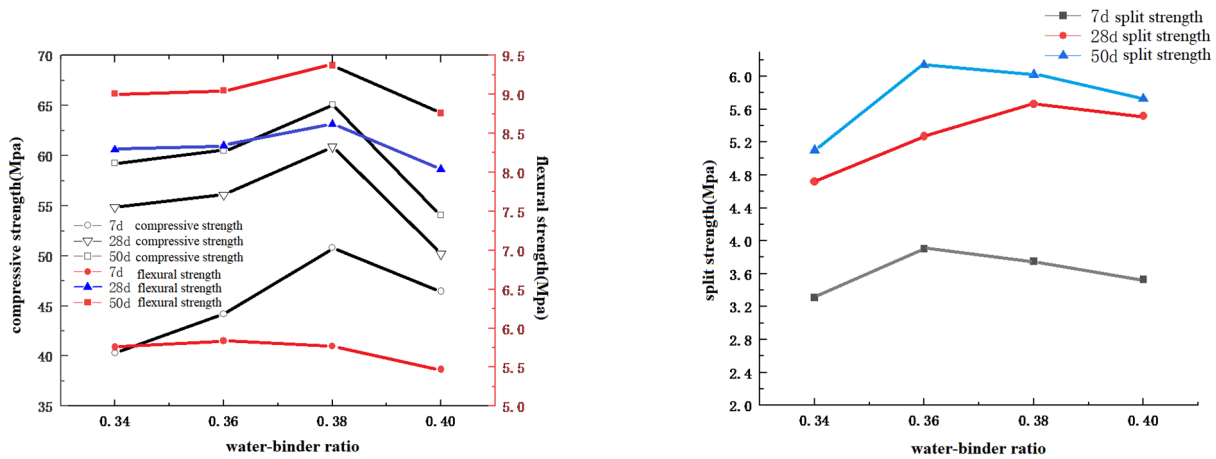
The impacts of different water-binder ratios, fly ash contents, water-reducing agent dosage and steel fibre contents on the spray performance of WSSFHTHS (Yan 2021) (rebound rate, spray thickness) were shown in Figs. 5-8. These figures showed that as the water-binder ratio increased, the spray thickness of WSSFHTHS increased first and then declined. The rebound rate declined first and then increased. After the wind pressure strength increased, the spray thickness and rebound rate changed similarly. A comparative analysis of the four figures showed that when the water-binder ratio was 0.38, it was more suitable for WSSFHTHS spray to reduce construction materials used. However, when the dumping time increased, the rebound rate of WSSFHTHS increased, and spray thickness declined. When the water-binder ratio was lower than 0.34, WSSFHTHS had greater friction and could easily cause the blockage of pipes in construction. When the water-binder ratio was 0.34~0.38, it had a better spray performance.

As the fly ash content increased, dumping time declined.

When the fly ash content was 10%, the spray thickness maximized at 262 mm. When the fly ash content was 30%, the rebound rate of shotcrete was minimized to 6.02%. As the wind pressure increased, the shotcrete rebound rate increased. Nevertheless, as the fly ash increased, the rebound rate declined. As the water-reducing agent dosage increased, dumping time declined. When the wind pressure was 0.9 MPa, the water-reducing agent dosage was 0.6%, the spray thickness maximized at 254 mm, and the rebound rate was 8.54 MPa.

As the water-reducing agent dosage increased, the spray thickness declined, and the rebound rate rose. When the wind pressure increased, the spray thickness and rebound rate increased. When the wind pressure was 1.1 MPa, the water-reducing agent dosage was 1.2%, and the spray thickness was 221 mm, reduced by 12.99%. The rebound rate was 13.77%, with a 61.24% increase.

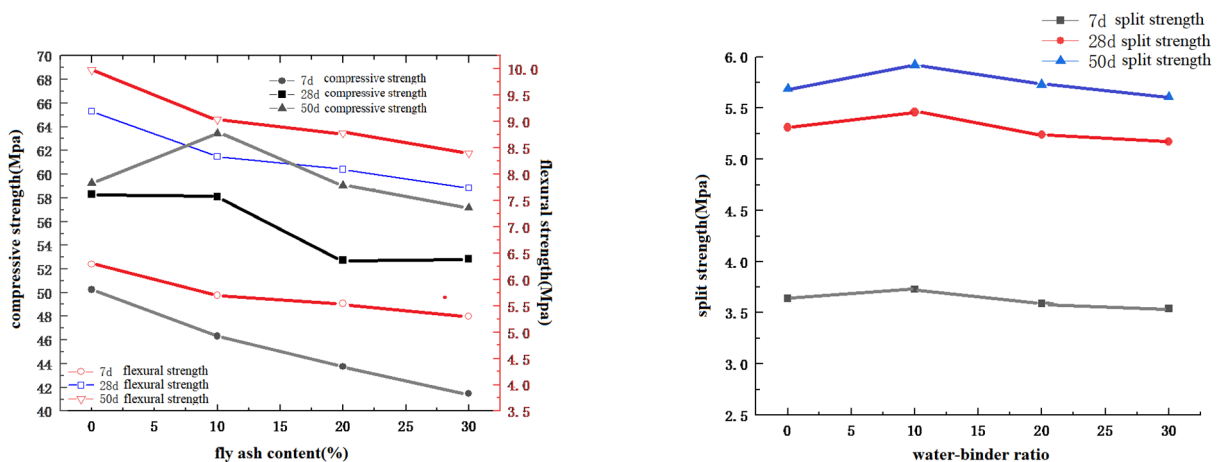
Adding steel fibre increased the spray thickness of WSSFHTHS and reduced its rebound rate. When the steel fibre content was 35 kg/m³, the spray thickness was 257



(a) Effect of different water binder ratios on flexural and compressive strength

(b) Effect of different water binder ratio on splitting tensile strength

Fig. 9 Mechanical properties under different water-binder ratio conditions



(a) Effect of different fly ash content on flexural and compressive strength

(b) Effect of different fly ash content on splitting tensile strength

Fig. 10 Mechanical properties under different fly ash content

mm, and the rebound rate was 17.91%. When the steel fibre content was 50 kg/m³, the spray thickness is 263 mm, reduced by 4.37% slightly compared with that when the steel fibre content is 45 kg/m³; but the rebound rate slightly raised to 13.16%, up by 5.03%.

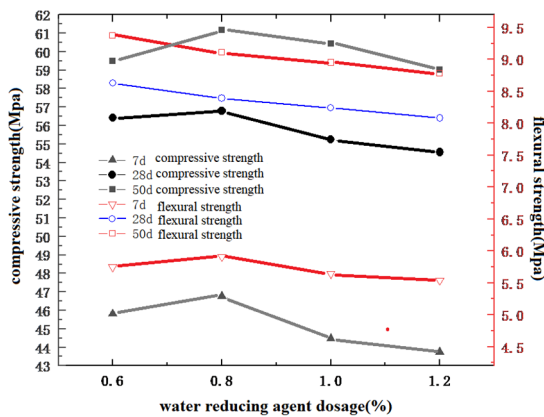
2.3.3 Basic mechanical property analysis

SYE-3000D electro-hydraulic testing machine, CSS-WAW1000 electro-hydraulic servo universal testing machine, and YAW-1000D microcomputer controlled electro-hydraulic servo compression and flexure resistant testing machine were adopted for the compressive strength, split strength and flexural strength tests followed GB/T50081 Standard for Test Methods of Concrete Physical and Mechanical Properties. The impacts of different water-binder ratios, fly ash contents, water-reducing agent dosage and steel fibre contents on the mechanical properties of WSSFHTHS (Jin *et al.* 2020) (flexural, compressive and splitting tensile strength) were shown in Figs. 9-12.

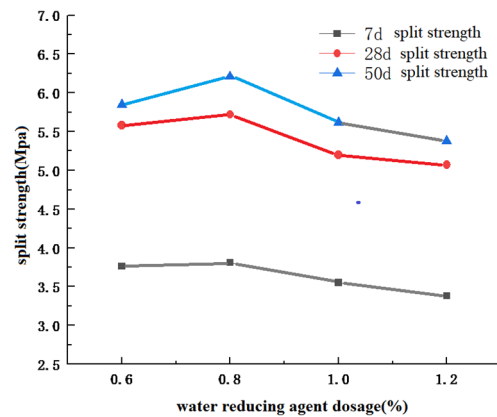
The above figures showed the impacts of the water-

binder ratio on WSSFHTHS mechanical properties: The water-binder ratio impacted most the compressive strength of WSSFHTHS, followed by the splitting tensile strength, and finally, the flexural strength. This was because the cement contents and hydration rates with different water-binder ratios were different. As a result, the compressive strength had significant differences. Besides, if the water-binder ratio was too high, the slurry content would also be increased, and the slurry could quickly fall at the nozzle. This made the spray hard. If the water-binder ratio was too high and the cement content reduced, it led to poor later strength of the sprayed-up concrete. When the water-binder ratio was 0.38, the maximum compressive strength of WSSFHTHS50d was 65.05 MPa.

Impacts of different fly ash contents on the mechanical property of WSSFHTHS: The results indicated that fly ash contents significantly influenced the compressive strength of WSSFHTHS, followed by the splitting tensile strength and flexural strength. The fly ash content significantly impacted the compressive strength. This was because the fly ash had a prolonged hydration reaction at the beginning,

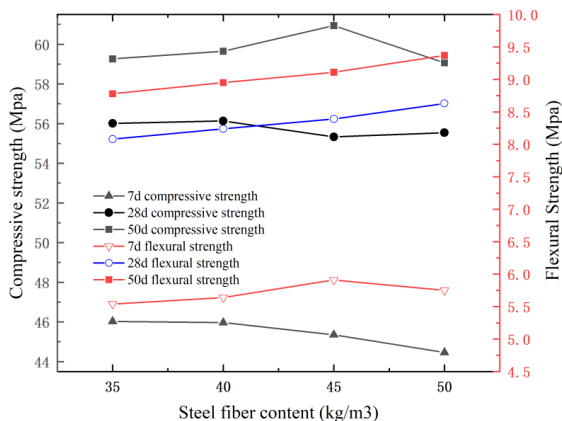


(a) Effect of different water reducing agent content on flexural and compressive strength

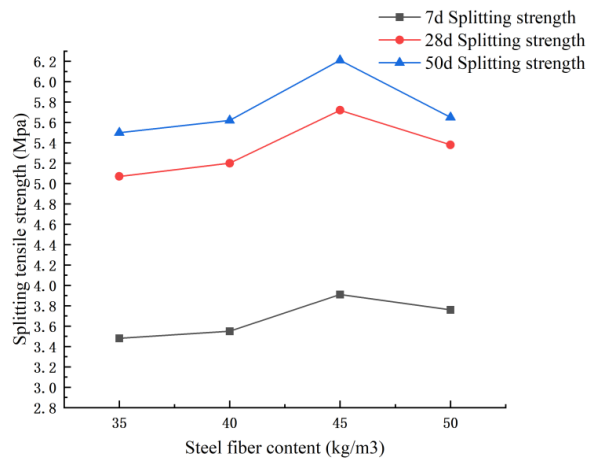


(b) Effect of different water-reducing agents on splitting tensile strength

Fig. 11 Mechanical properties of different water-reducing agent content



(a) Effect of different steel fibre content on flexural and compressive strength



(b) Effect of different steel fibre content on splitting tensile strength

Fig. 12 Mechanical properties under different steel fibre content

Table 2 Mix ratio of spray experiment

Material	Water (kg)	Cement (kg)	Silica fume (kg)	Fly ash (kg)	Water reducing agent (kg)	Steel fiber (kg/m ³)	Accelerator (%)	High titanium slag sand (kg)	High titanium slag stone (kg)
A1	136.8	375	50	75	3	45	7.2	627.1	736.2
Material	Water (kg)	Cement (kg)	Silica fume (kg)	Fly ash (kg)	Water reducing agent (kg)	Steel fiber (kg/m ³)	Accelerator (%)	Common sand (kg)	Common gravel (kg)
A2	136.8	375	50	75	3	--	7.2	788.2	925.3

Table 3 Test results of rebound rate and jet thickness under different jet wind pressure

Number	0.5 MPa	0.7 MPa	0.9 MPa	1.1 MPa	0.5 MPa	0.7 MPa	0.9 MPa	1.1 MPa
	Sspray thickness/mm				Rebound rate/%			
A1	154	201	257	238	21.82	13.91	5.83	8.92
A2	161	185	171	147	28.73	22.65	27.74	30.21

and when a considerable amount of fly ash was added to replace cement, the cement hydration products reduced at the beginning. As a result, the early strength of WSSFHTHS diminished. When the fly ash content ranged between 10% and 20%, the mechanical property of WSSFHTHS was the best. Its maximum 50 d compressive strength was 63.45 MPa.

Impact of different water-reducing agent contents on the mechanical property of WSSFHTHS: The water-reducing agent significantly influenced the compressive strength of SFHSWS, followed by splitting tensile strength and bending strength. This was because when the water-reducing agent dosage was small, the workability of WSSFHTHS could be improved. It improved carrier uniformity and compactness. Besides, it allowed the cement to disperse effectively in mixture to enhance the hydration rate of grout, thereby improving the mechanical property of WSSFHTHS from various aspects. When the water-reducing agent dosage was 0.8%, the maximum splitting tensile strength of WSSFHTHS50d was 6.21 MPa.

Impacts of different steel fibre contents on WSSFHTHS mechanical property: The steel fibre contents had the most significant influence on the compressive strength of WSSFHTHS, followed by the splitting tensile strength and flexural strength. This was because when the steel fibres were distributed in shotcrete, they could pull and prevent the concrete on both sides from spreading when the test piece had cracks and prevent further cracks, thereby increasing the flexural strength and tensile strength WSSFHTHS. The most significant change was that after adding steel fibres, the original brittle failure of the typical wet shotcrete could be changed to ductile fracture (Hemphill 2013). When the steel fibre content was 45 kg/m³, the mechanical property of WSSFHTHS was the best, and the maximum 50 days split strength and flexural strength were 6.60 MPa and 9.72 MPa, respectively.

2.3.4 Optimal mix ratio of WSSFHTHS

In conclusion, the orthogonal test method was adopted for the test and comprehensive data analysis of the work performance (slump, cohesiveness, and water retention property), the performance of spray (rebound rate and spray

thickness) and basic mechanical properties (compressive strength, flexural strength, and split strength) of WSSFHTHS when the contents of four factors (water-binder ratio, fly ash, water reducing agent, and steel fibre) were different. The optimum mix ratio of WSSFHTHS was water-binder ratio at 0.38, 15% fly ash content and 0.8% water reducing agent dosage, and 45 kg/m³ steel fibre.

3. Optimization study on WSSFHTHS spray technology

3.1 Optimization study on the jet wind pressure and jet thickness of WSSFHTHS

3.1.1 Impacts of wind pressure on rebound rate and jet thickness

The jet wind pressure values used were 0.5 MPa, 0.7 MPa, 0.9 MPa and 1.1 MPa, respectively. To compare the rebound rate and jet thickness of WSSFHTHS of the optimum mix ratio with typical wet shotcrete and the impacts (Wang *et al.* 2012) of different wind pressure values on rebound rate, jet thickness and the optimal jet wind pressure, this study experimented with different mix ratio per Table 2, and the experiment result was recorded in Table 3.

Table 3, Figs. 13 and 14 show an appropriate jet wind pressure for construction. The primary jet thickness increases first and declines as the jet wind pressure rises, and the rebound rate decreases accordingly. Common wet shotcreting also has the same phenomena, but the increase in the jet thickness and the decrease in the rebound rate of WSSFHTHS are more significant than those of common wet shotcrete. When the wind pressure is 0.7 MPa, the rebound rate of wet shotcrete is minimum, and its jet thickness is maximum at 22.65% and 185 mm, respectively. When the jet wind pressure is 0.9 MPa, the rebound rate of WSSFHTHS is the minimum, and its jet thickness is the maximum at 5.83% and 257 mm, respectively. Compared with common wet shotcrete, its spray performance is greatly improved.

The above experiment result shows that adding steel

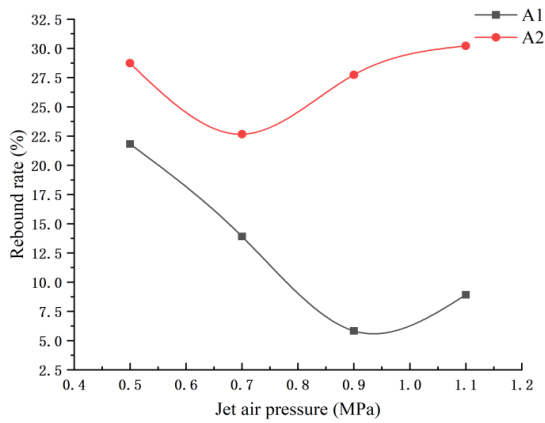


Fig. 13 Influence of jet air pressure on rebound rate

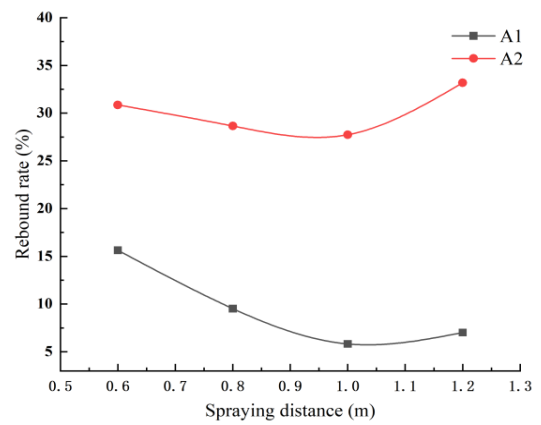


Fig. 15 Influence of jet air pressure on rebound rate

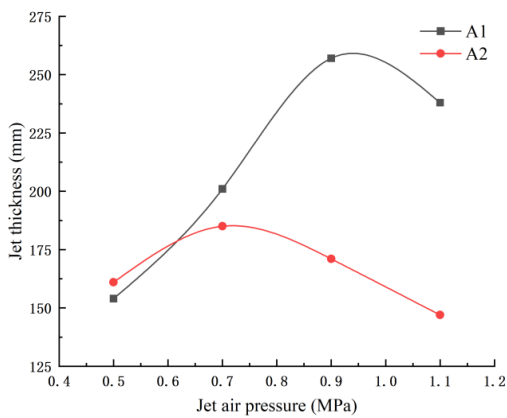


Fig. 14 Influence of jet wind pressure on the jet thickness

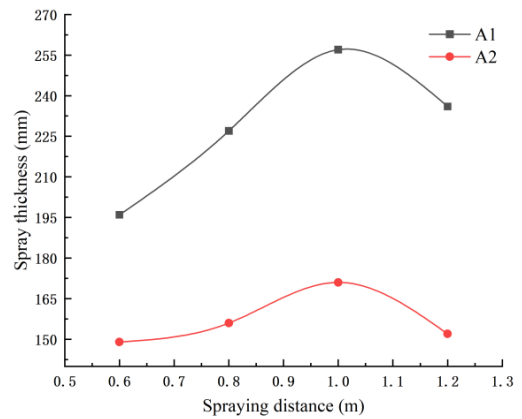


Fig. 16 Influence of jet wind pressure on the jet thickness

fibres can effectively increase the jet thickness of WSSFHTHS and reduce its rebound rate under appropriate wind pressure. Compared with the common wet shotcrete, high titanium heavy slag and steel fibres increase the friction force. After jet wind pressure increases, the jet thickness can be effectively improved, and the rebound rate can be effectively reduced. Besides, because high titanium heavy slag is lighter than typical gravel, the time of fall caused by the gravity force, more significant than the bond with the sprayed surface, is postponed. Moreover, with the bonding action of steel fibres, the jet thickness of WSSFHTHS significantly increases, and its rebound rate can be effectively reduced. Lower wind pressure is unsuitable for WSSFHTHS and worsens the spray performance.

3.1.2 Impact of the spray distance on the rebound rate and spray thickness

Spray distance refers to the distance from the nozzle to the sprayed surface. Based on the impact of jet wind pressure on the rebound rate and spray thickness discussed in the former section, in this section, the study will focus on the effects of the spray distance on the rebound rate and spray thickness of WSSFHTHS to find out the optimal spray distance. The spray distance is 0.6 m, 0.8 m, 1.0 m, and 1.2 m, respectively. The mix ratio in the experiment is shown in Table 2, and the experiment result is recorded in Table 4.

Table 4 and Figs. 15 and 16 show that the impact of spray distance on the performance of the spray of common wet shotcrete is smaller than that of WSSFHTHS. As the spray distance increases, the spray thickness increases and then declines. The rebound rate drops first and then increases. The growth and decrease in the rebound rate do

Table 4 Test results of rebound rate and spray thickness under different jet wind pressure

Number	0.6 m	0.8 m	1.0 m	1.2 m	0.6 m	0.8 m	1.0 m	1.2 m
	Spray thickness/mm				Rebound rate/%			
A1	196	227	257	236	15.64	9.52	5.83	7.02
A2	149	156	171	152	30.86	28.65	27.74	33.17

not vary greatly, but the impact on the spray thickness of WSSFHTHS is more significant than that of common wet shotcrete. When the spray distances are 0.6 m, 0.8 m, 1.0 m and 1.2 m, the spray thickness is 196 mm, 227 mm, 257 mm, and 236 mm, and the rebound rates are 15.64%, 9.52%, 5.83%, and 7.02%. The spray thickness and rebound rate of common wet shotcrete are 149 mm, 156 mm, 171 mm and 152 mm, respectively. The rebound rates are 30.86%, 28.65%, 27.74% and 33.17%, respectively. The impacts of spray distance on WSSFHTHS are more significant than ordinary concrete.

The above experiment result shows that adding steel fibres effectively reduces the rebound rate of WSSFHTHS with an appropriate distance. Similar to the reasons mentioned in the former section, the bonding action of steel fibres can effectively mitigate the rebound rate of WSSFHTHS. Too long or short a spray distance affects the spray performance.

4. Engineering application

In this paper, Ansys finite element analysis software is used for simulation analysis, and then construction quality control is put forward in engineering applications. The WSSFHTHS developed is used in the lining works of 3 tunnels of Zhonggouwan tailing pond to study its safety. The maximum excavation width of the tunnel in the study is 3 m, and its excavation height is 2.8 m.

4.1 Calculation model and selection of parameters

4.1.1 Calculation model

The model is selected based on the impacts of tunnel excavation on boundary conditions. The circle's centre

corresponds to the circular arc of the tunnel is taken as the origin of coordinates, and Y is the dead-weight direction of the rock. The distance from the walls on both sides of the tunnel to the calculation boundary is 35 m, the bottom of the buried depth is taken to -30 m, and the top is three times the diameter of the hole. The boundary constraint of the model is a horizontal displacement constraint; the bottom has a perpendicular constraint boundary on the left and right sides, and there is a horizontal constraint boundary perpendicular to the tunnel axis. The upper surface is natural. Initial conditions: The stress field generated by the dead weight is taken as the primary stress field. In the calculation, the stratum is an isoparametric elastoplasticity plane PLANE82. The lining supporting structure of WSSFHTHS adopted a two-dimensional beam element BEAM3. A rock bolt is a rod unit LINK1 (Zhu 2009).

A mechanical model is established using ANSYS based on the above (Alawadhi 2015). The model grid is shown in Fig. 17.

4.1.2 Selection of material parameters

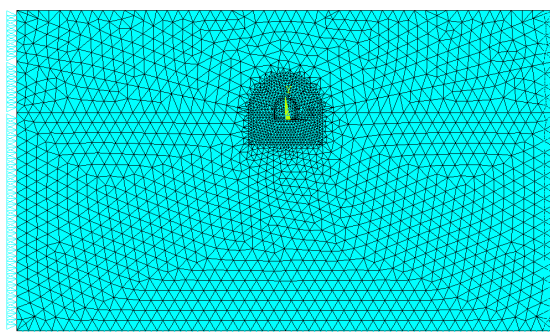
In this section, the rock in the simulation construction section is level IV rock. For the structural analysis under the former support conditions, the equivalent material method is adopted to simulate the surrounding rock reinforced with advanced rock bolts. After conversion, the concrete modulus of elasticity (Yu 2005) can be obtained according to the equivalent stiffness principle in formula (1).

$$E = E_0 + \frac{S_g \times E_g}{S_c} \tag{1}$$

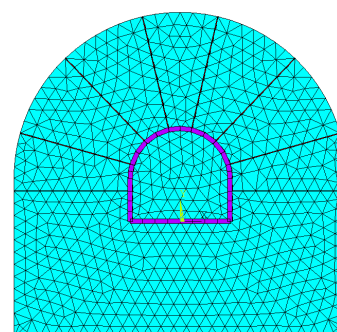
Where

E — Modulus of elasticity after conversion;

E_0 — Former modulus of elasticity of concrete;



(a) Overall finite element calculation model grid



(b) Detailed finite element calculation model grid

Fig. 17 Finite element calculation model

Table 5 Surrounding rock and supporting parameters

Material	Parameter	Elastic modulus	Poisson's ratio	Density	Internal friction angle	Cohesion
		$E/(GPa)$	μ	$\rho (kg/m^3)$	$\phi(^\circ)$	C/MPa
Level IV surrounding rock		5.0	0.25	2570	36	0.21
Shotcrete		33.6	0.20	2400	-	-
$\phi 25$ Mortar anchor		203.0	0.30	7930	-	-

- S_g — Sectional area of steel;
- E_g — Modulus of elasticity of steel;
- S_c — Sectional area of concrete

For the structural analysis of steel centring, mesh reinforcement, sprayed concrete and advanced grouting support, the form of support is simplified as follows: The equivalent material method is adopted, in which the steel centring and mesh reinforcement can be taken as a new material, and the material parameters are calculated following the equivalent stiffness principle. The elasticity modulus of WSSFHTHS can be obtained through a lab test. The values of other formation parameters can be taken according to the recommended values provided in the reconnaissance report and GB/T 50218. The parameters are shown in Table 5.

4.1.3 Pre-design of WSSFHTHS lining support

An optimal WSSFHTHS lining thickness was designed using ANSYS through iterative calculation to play the role of WSSFHTHS lining in flexible support. That stabilized the tunnel surrounding rock, and the lining would not be damaged. The iterative calculation of thickness R was conducted through the ANSYS function to get the optimal lining R.

- (1) Design variable: the scope of control of lining thickness R was 0.05 m ~ 0.10 m.
- (2) Objective function: Significant tunnel deformation includes roof deformation, sidewalls, and intrados. According to the regulations (Lu 2018, Luo 2018), the convergence value of the peripheral permissible relative displacement should be

$$0.15\% \leq (RDB, RLB) \leq 0.5\%.$$

$$RDB = \frac{\zeta_B + \zeta_D}{h}, \quad RLB = \frac{\varepsilon_B + \varepsilon_L}{B} \quad (2)$$

Where

- RDB — Relative displacement of tunnel roof and intrados (%);
- ζ_B — Displacement of tunnel intrados (mm);
- ζ_D — Displacement of tunnel roof (mm);
- h — Tunnel height (m);
- RLB — Relative displacement of two tunnel sides (%);
- ε_B — Displacement of the tunnel wall on the left (mm);
- ε_L — Displacement of the tunnel wall on the right (mm);
- B — Tunnel span (m).

Major control points are shown in Fig. 18. The design values of the tunnel and inclined shaft bolting and shotcrete support was specified in GB/T 50086 Technical Code for Engineering of Ground Anchorages and Shotcrete Support are shown in Table 6.

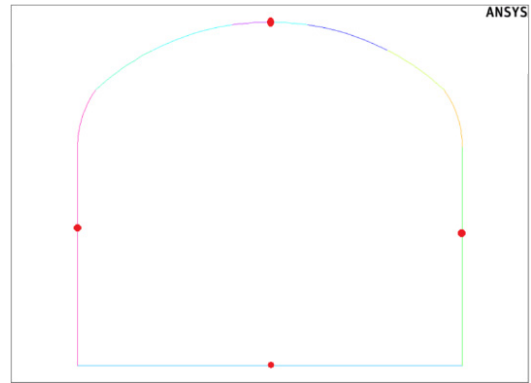


Fig. 18 Location of main control points

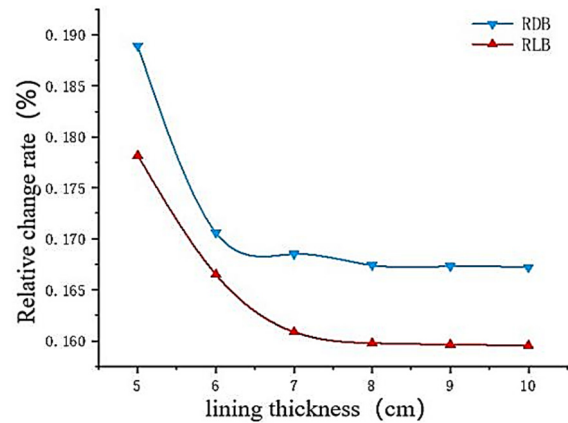


Fig. 19 Change curve of relative displacement convergence value

- (3) State variable: for the convenience of calculation, the tunnel support thickness was uniform. When the cross-sectional shotcrete area was the smallest, the lining thickness R was the smallest. From the iterative calculation of the lining thickness R using the Ansys function, the change curve of the convergence value of relative displacement of tunnel roof, intrados and side walls is shown in Fig. 19 below.

From Fig. 19, the relative displacement of the tunnel roof, intrados, and side walls declined first and then became stable. RDB decreased from 0.1889% when the support thickness was 5 cm to 0.1685% when the support thickness was 7 cm. Then it becomes stable. RLB declined from 0.1782% when the support thickness ranged from 5 cm to 0.1598% when the support thickness was 8 cm. Then it became stable. The greater the support thickness, the greater the rigidity, the more substantial the restraints on the surrounding rock, and the smaller the deformation. In such a case, the rate of change would be stable.

Table 6 Design values of tunnel bolting and shotcrete support

IV surrounding rock cavern span		$B \leq 5 m$
Standardize support measures	The thickness of reinforced mesh shotcrete is R = 8 cm, the length of the low-prestressed bolt is L = 1 cm, and the spacing is between 1 m and 2 m.	

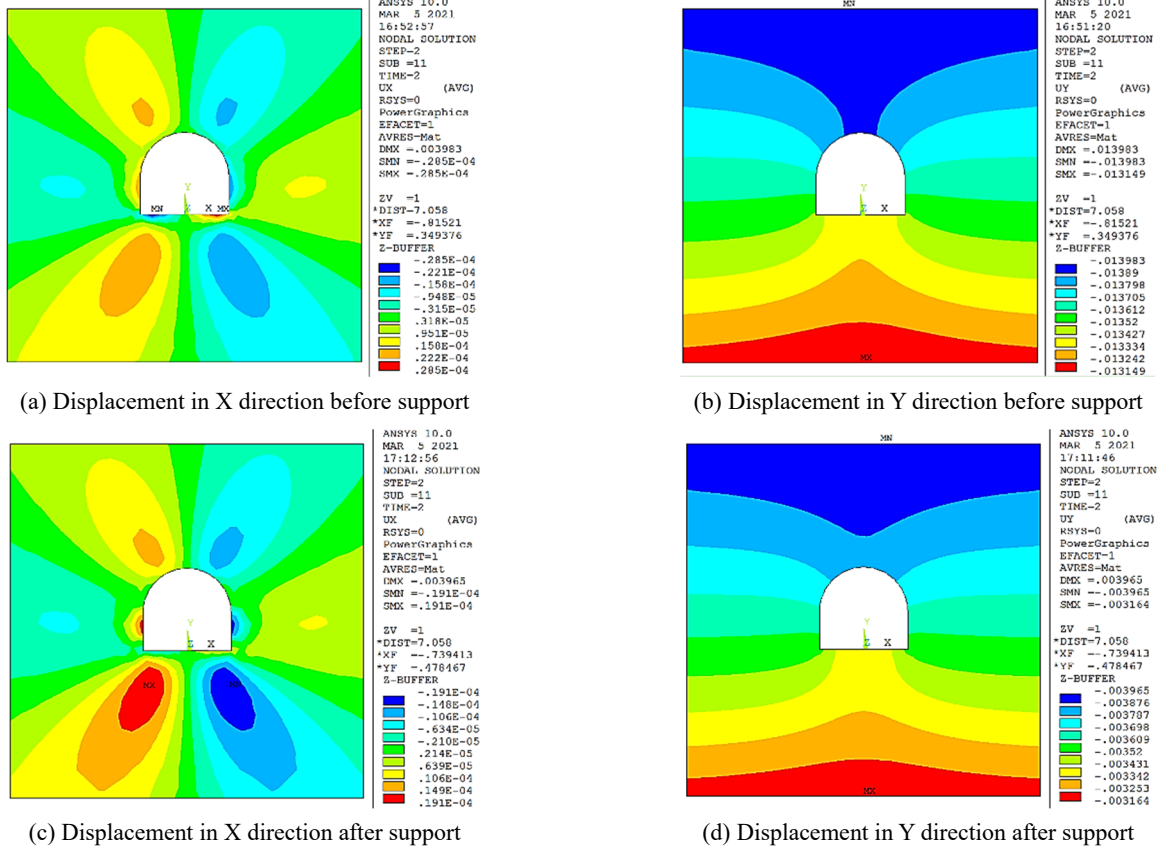


Fig. 20 Contrast cloud diagram of displacement before and after support

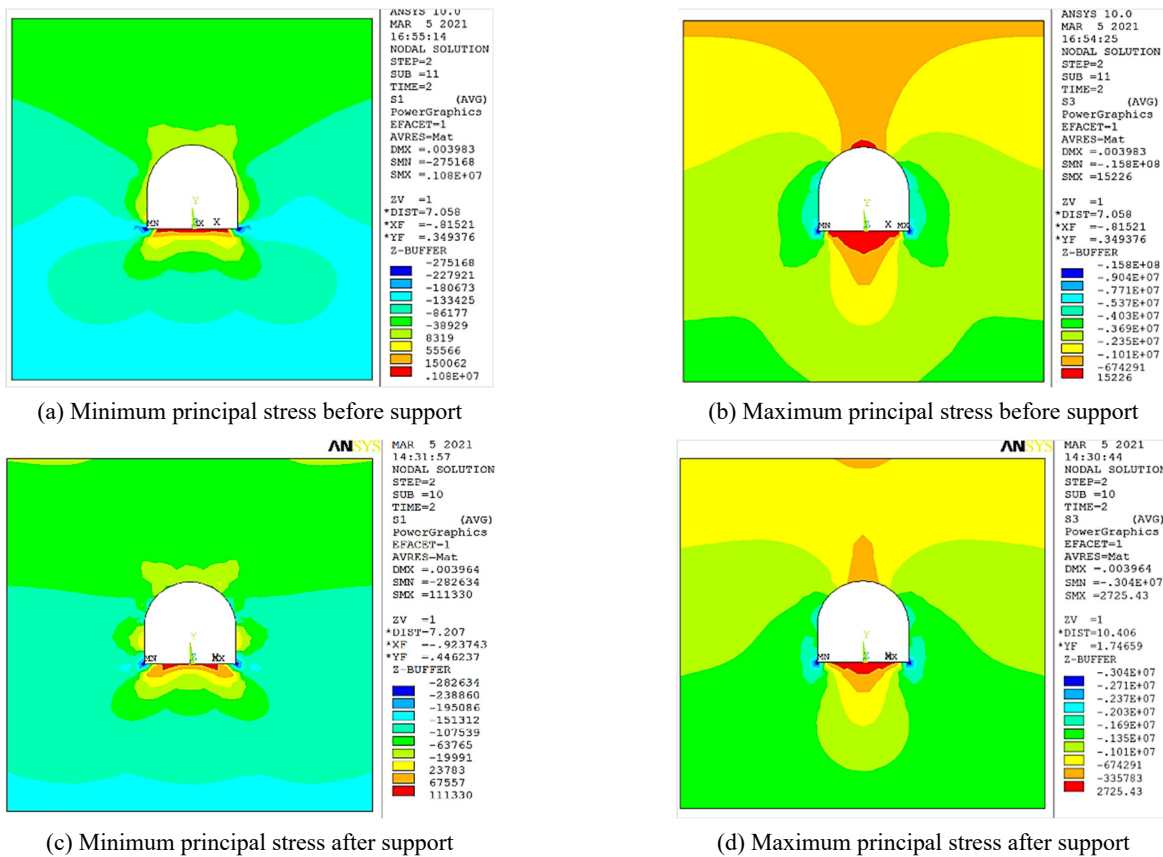


Fig. 21 Contrast cloud diagram of stress before and after support

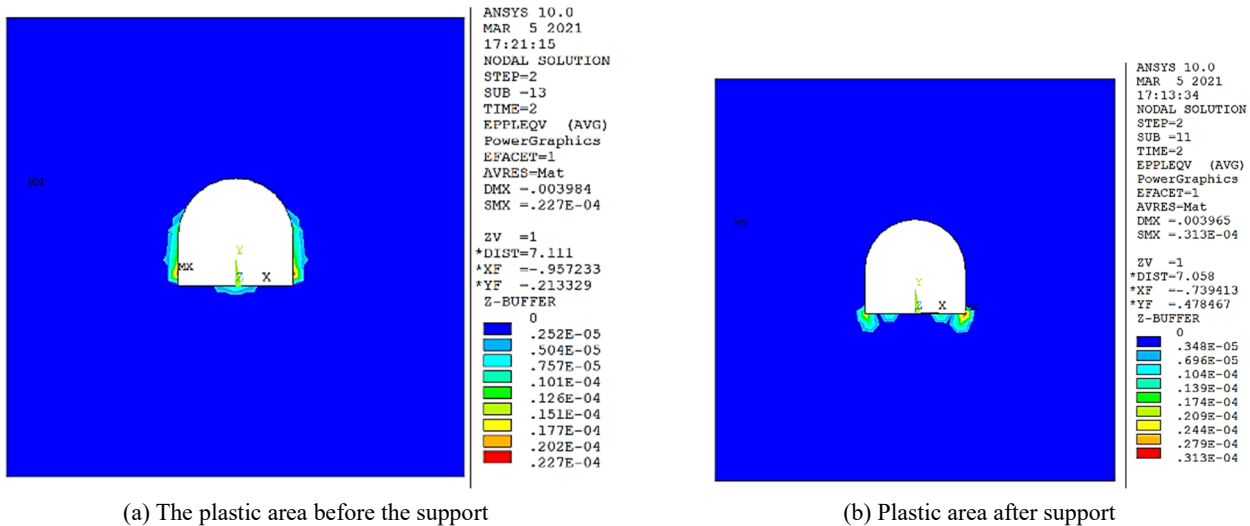


Fig. 22 Contrast cloud map of the plastic area before and after support

According to the design value specified in the code, with the required strength and surrounding rock stability, WSSFHTHS lining had a thickness of 80 mm, which was the optimal lining thickness in this case in the study.

4.2 Analysis of numerical simulation result

Figs. 20-23 show the stress distribution in the displacement field of the cavern, main stress field, plastic area and support obtained according to the above conditions and method through calculation via adopting the lining support after tunnel excavation and WSSFHTHS bolting and shotcrete support is adopted.

4.2.1 Analysis of displacement field before and after tunnel excavation support

Fig. 20 shows that before the support after tunnel excavation and after WSSFHTHS bolting and shotcrete support, the horizontal displacement of the tunnel surrounding rock was smaller than the vertical displacement. Before and after the support, the displacement of the tunnel surrounding the rock in X (horizontal) direction was smaller than 1 mm. After adopting WSSFHTHS bolting and shotcrete support, the displacement in X direction slightly declined, showing that tunnel construction did not affect the horizontal displacement of surrounding rock much. The depression area caused by excavation disturbance took approximately the shape of a funnel. The further from the tunnel centre line, the smaller the impact. The calculation result agrees with the stratum deformation law during the construction of the underground cavity. After tunnel excavation, the model's most extended horizontal displacement appeared near the tunnel's haunch, and the right and left haunches were symmetric. After excavation, the rock excavation had a slightly significant impact on the part surrounding the rock. The support and constraint function of the part surrounding rock disappeared, and the roof became loose. The tunnel lost its support vertically and collapsed due to gravity. The tunnel bottom bended upwards under the action

of additional stress. The maximum stratum settlement of the surrounding rock with initial displacement in the Y direction before support was 13.98 mm. After adopting WSSFHTHS bolting and shotcrete support, the maximum settlement displacement became 3.97 mm.

4.2.2 Stress analysis before and after tunnel excavation support

After tunnel excavation, deformation and stress were released in the surrounding rock, changing the original stress field. Before tunnel excavation support, the minimum principal stress was 1.08 MPa, mainly distributed at the tunnel intrados (Fig. 21). The maximum principal stress was -15.8 MPa before support, primarily spread in the tunnel's two sidewall corners. Stress concentrated at the spatial angle outside the straight tunnel wall, and a compression stress concentration area formed on the arch. From Fig. 21, shearing failure quickly appeared at the straight wall toe in tunnel excavation, which agreed with what was observed on site. A comparison of stress calculation results before and after tunnel excavation support in the model showed that adopting WSSFHTHS bolting and shotcrete support improved the surrounding rock's maximum and minimum principal stress distribution. The minimum principal stress of the surrounding rock dropped from 1.08 MPa before support to 0.11 MPa. The maximum principal stress also dropped from -15.8 MPa to -3.04 MPa. The calculation results' maximum and minimum principal stresses were smaller than the extreme compressive strength and tensile strength of WSSFHTHS in the test. The supporting structure formed with WSSFHTHS and advanced rock bolt gave full play to the surrounding rock's self-supporting capacity and the systematic rock bolt's tensile and deformation restrained capacity. Combined with the original tensile strength and preferable deformation restrained capacity of WSSFHTHS, the deformation modulus and amount of deformation of surrounding rock and supporting structure could be effectively improved. Owing to the poor bulking property of the surrounding rock, the lining at the sidewall corners shall be specially reinforced during

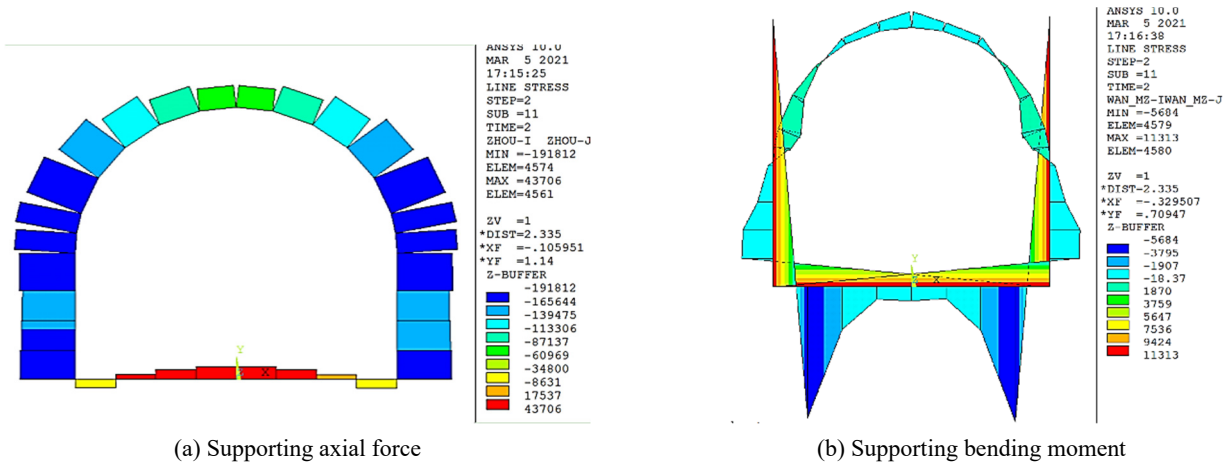


Fig. 23 Cloud diagram of internal force of tunnel supporting structure

construction.

4.2.3 Comparison of plastic areas before and after tunnel excavation support

The mechanical mechanism for suppressing the instability of surrounding rock in tunnel excavation (Jiang *et al.* 2022, Yan *et al.* 2020) enhanced the structural strength of lining support and restricted the development of plastic areas around the tunnel after excavation. After excavation, plastic areas of surrounding rock were distributed on tunnel side walls and in the middle of the intrado, the major range of the plastic regions of surrounding rock was approximately within 3 m (Fig. 22). The plastic area became gradually more prominent from the arch foot of the tunnel to the side walls. The maximum value of the plastic area is 1.572 mm, which appeared on both sidewalls. There were no plastic areas on the roof and foot. After adopting WSSFHTHS bolting and shotcrete support, the plastic areas on the sidewalls disappeared, and there was only a plastic area at the sidewall toe.

The supporting structure formed using WSSFHTHS and advanced rock bolt effectively slowed down and improved the instability of the cross-section after tunnel excavation and shrank the plastic area to the wall toe after shearing, thereby effectively improving the working conditions of the tunnel. Besides, rock bolt yield usually appeared as the shearing failure between the bolted section and the grout. The numerical simulation result showed that the rock bolt is still in good condition as the stress was released and had no yield.

4.2.4 Internal force of the supporting structure analysis

Calculating the internal structural strength of the lining mainly involved bending moment and axial force. After excavation, it could be calculated according to the axial force distribution and the bending moment after WSSFHTHS lining support, as shown in Fig. 23.

Fig. 23(a) shows that after tunnel excavation, with WSSFHTHS bolting and shotcrete support, the axial force distributes in a sub-elliptical form. The maximum axial force was -191.812 kN/43.706 kN, and the maximum

bending moment was 5.684 kN.m /11.313 kN.m. The maximum bending moment mainly appeared at the sidewall corners. The maximum axial force was concentrated at the arch foot, sidewalls, and the middle of the intrados. Because the maximum bending moment and the maximum axial force were not on the same cross-section, the internal force of the roof supporting structure was small, showing that the surrounding rock pressure on the lining was minimized. There was no inverted arch construction, so tension stress might be concentrated at the sidewall toe and intrados, which could easily lead to partial failure and would not be suitable for the overall stability of the supporting structure. The lining supporting structure was a WSSFHTHS spray thin-wall case that could be suitable for structural bending resistance. It could meet the requirements of the self-organizing contour formed after tunnel excavation and ensure the safety and stability of the surrounding rock (Shaposhnik 2018).

4.3 Construction quality control

4.3.1 Mixing and transportation of WSSFHTHS

When a forced agitator is adopted for stirring wet materials, the charging sequence and mode shall be revised to ensure a uniform distribution of steel fibres in the wet mixture. The one-time mixing amount shall not exceed 80% of the rated mixing amount. The materials should be added in three batches: sand with high titanium heavy slag, stone with high titanium heavy slag, cement, mineral admixture, and steel fibre. The additives shall be mixed evenly with 20%~50% water for mixing and then add to the mixed dry material. The coarse and fine aggregate contained high titanium heavy slag, cement, mineral admixture, and steel fibre, which should be mixed dryly for 2-3 minutes in the forced agitator and then mixed for 3-4 minutes after adding water-reducing agent and mixing water. The mixed-up WSSFHTHS possesses preferable workability to meet the slump requirement. After preparing WSSFHTHS, it should be transported to the construction site for spray construction as soon as possible, stirred constantly during transport to avoid segregation, bleeding and reduce slump, and consolidation. After mixing WSSFHTHS, it should not be

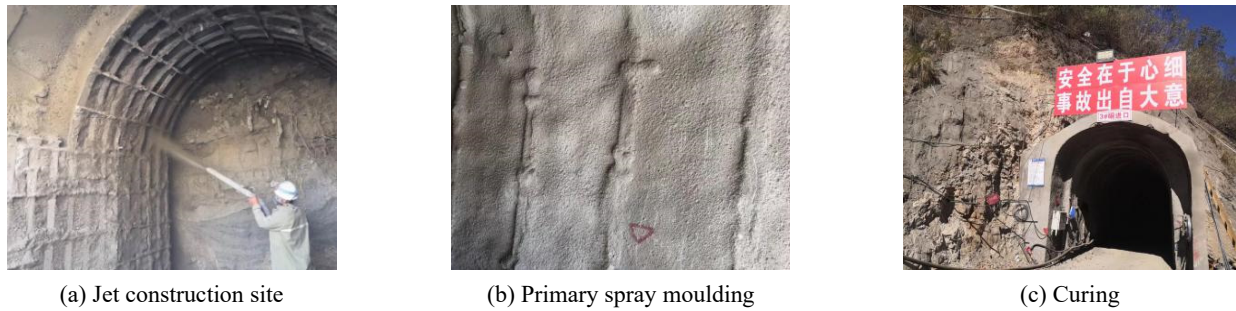


Fig. 24 Site construction and maintenance diagram

stored for more than two hours. Sufficient loading staff shall be assigned to ensure continuous and homogeneous loading if it was loaded manually.

4.3.2 Spray operation

The spray could be conducted in sections or subdivisions according to construction conditions (Topçu and Bilir 2010). The wind pressure shall be controlled to be 0.9 MPa during shotcrete spray. The nozzle shall be kept as vertical as much to the construction operation plane. The manual spray distance shall be kept at about 1 m, making the WSSFHTHS lining compact and homogeneous, reducing the rebound rate, and saving construction cost. If a thick spray layer is required, layers can form to make the shotcrete form a homogeneous layer. It shall not be sprayed at one time to reach the designed thickness. It is better to spray the later layer one hour after spraying the former layer's. During spraying, WSSFHTHS jetted out shall not form blocks moving down on the construction surface, nor shall it be too thin and flow down. If there are such problems, they shall be removed and resprayed. After the initial set of WSSFHTHS, the excessive thickness shall be removed timely using a darby or scraper, and then the surface shall be troweled. If the spray plane is natural and levelled, it will improve the overall stress and durability.

Engineering practice shows that if a plastic layer of about 50 mm is formed on the sprayed surface, WSSFHTHS coarse aggregate can be embedded better. To reduce the rebound rate, the WSSFHTHS layer sprayed at one time shall not be too thin or too thick. Otherwise, it will affect the cohesion of WSSFHTHS. According to the finite element simulation calculation result, the design thickness of WSSFHTHS lining is 80 mm. It can be formed in several layers. The one-time spray thickness shall be 30~50 mm. During layered spray, the later layer shall be sprayed one h after the final set of the former layer. If the latter layer is sprayed before the last set of the former layer, the former WSSFHTHS layer's structure may be disturbed, causing hollowness and even drop-out of the spray layer and affecting the lining safety.

4.3.3 Lining curing

The characteristic of drying shrinkage of concrete may cause cracks in the concrete structure, thereby affecting its impermeability and durability (Ahmed and Ansell 2014). The water-binder ratio of WSSFHTHS is low, and there are many unhydrated cement particles in the lining structure,

which can, to a certain extent, inhibit drying shrinkage, thus affecting tunnel safety. The curing of WSSFHTHS lining shall be strengthened. Lining curing can be begun two hours after the final set of the spray layer. Before curing, the structural surface shall be wet by spraying or film coverage. The curing time shall be 10~14 d. When the relative environmental humidity is greater than 85%, natural maintenance shall be adopted. When the ambient temperature is lower than +5°C, curing by sprinkling shall not be adopted.

The construction process and the curing effect are shown in Fig. 24. The construction and curing effect are good. There are no cracks, hollowness or drop-out, which has verified the construction operability of WSSFHTHS.

4.3.4 AI and tunnel detection

Tunnel lining quality check encounters new opportunities and challenges with intelligence development worldwide. In the future, based on ANSYS, we can combined with AI image recognition to detect tunnel lining cracks to further reduce cost and improve efficiency (Gao 2021). Besides, tunnel intelligent detection robot carries laser equipment or camera that can be used to detect abnormal temperature alarm simultaneously (Chen 2020). Mansoor (Mansoor and Zhang 2012) used a knowledge-based artificial intelligence system to diagnose tunnel lining crack damage. It provides a certain basis for making technical decisions on diagnosing crack damage in the second section of tunnel lining. The intelligent monitoring and detection method combined with the smart era can save a lot of human resources, improve the accuracy and feasibility of tunnel detection, and has excellent social and economic benefits.

5. Conclusions

This paper studied the impacts of different water-binder ratios, fly ash contents, steel fibre contents, and water-reducing agent dosage on WSSFHTHS work performance, the performance of spray, and basic mechanical properties. It optimized the construction technology of WSSFHTHS with an optimum mix ratio according to spray technology and based on a comparison with common wet shotcrete. It stimulated the optimum thickness of WSSFHTHS lining and the stability of supporting structure and surrounding rock using ANSYS, put forward the construction quality

control points of WSSFHTHS, and applied WSSFHTHS on three sites to verify its engineering use safety.

Major research conclusions include:

- (1) The test and comprehensive data analysis of the work performance (slump, cohesiveness, and water retention property), the performance of spray (rebound rate and spray thickness) and basic mechanical properties (compressive strength, flexural strength and split strength) of WSSFHTHS were conducted. The optimum mix ratio of WSSFHTHS was: water-binder ratio at 0.38; the fly ash content at 15%; 0.8% of water reducing agent; and 45 kg/m³ of steel fibre.
- (2) When the jet wind pressure was 0.9 MPa, the rebound rate of WSSFHTHS was minimized, and its jet thickness maximized at 5.83% and 257 mm, respectively. The spray distance affected the spray thickness of WSSFHTHS, and the optimal spray distance was 1.0 m.
- (3) The iterative calculation through ANSYS showed that the optimal lining thickness of WSSFHTHS was 80 mm.
- (4) The displacement field, stress field, and plastic area of the surrounding rock-supporting structural system and the distribution and change of the internal force of the supporting structure were analyzed. The result showed that after WSSFHTHS lining is used, displacement of the tunnel surrounding rock greatly improved, and the development of plastic areas was effectively controlled.
- (5) WSSFHTHS construction quality control measures were implemented from mixing and transportation, spray operation, and lining curing.
- (6) WSSFHTHS was applied on three sites for a trial. The support effect was good, and there were no cracks, hollow and drop-out, which was similar to the numerical simulation result.

Acknowledgments

This study was financially supported by “Research Fund of University Students’ Innovation and Entrepreneurship Project”: Research on Mechanical Properties of Wet Shotcreting Mixed with Steel Fibre and High Titanium Heavy Slag (S202011360019) and Ph.D. Starting Research Fund: Research on the Technology and Industry of a New Type of Prefabricated High-Titanium Heavy Slag Concrete Composite Board (no. 035200192).

References

Ahmed, L. and Ansell, A. (2014), “Vibration vulnerability of shotcrete on tunnel walls during construction blasting”, *Tunnell. Undergr. Space Technol.*, **42**, 105-111.
<https://doi.org/10.1016/j.tust.2014.02.008>

Alawadhi, E.M. (2015), *Finite Element Simulations Using ANSYS*, Second Edition, CRC Press.
<https://doi.org/https://doi.org/10.1201/b18949>

Chen, X. (2020), *Face Stability and Reinforcement of the Tunnel in Weak Surrounding Rock*, Geotechnical and Geological Engineering.

Dai, C., Jiang, K. and Wang, Q. (2020), “Recognition of Tunnel Lining Cracks Based on Digital Image Processing”, *Mathe. Probl. Eng.*, **2020**, 5162583.
<https://doi.org/10.1155/2020/5162583>

Ding, M.Q. *et al.* (2019), “Study on The Influence of Polycarboxylate Water-Reducing Agent Content on Concrete Performance”, *Fujian Transportation Technology*, **6**(1). [In Chinese]

Duarte, G., Bravo, M., de Brito, J. and Nobre, J. (2019), “Mechanical performance of shotcrete produced with recycled coarse aggregates from concrete”, *Constr. Build. Mater.*, **210**, 696-708. <https://doi.org/10.1016/j.conbuildmat.2019.03.156>

Gao, X. (2021), “Tunnel lining crack detection technology under the background of artificial intelligence”, *Northern Commun.*, 92-94. <https://doi.org/10.15996/j.cnki.bfjt.2021.11.023>

Guler, S. and Akbulut, Z.F. (2022), “Residual strength and toughness properties of 3D, 4D and 5D steel fiber-reinforced concrete exposed to high temperatures”, *Constr. Build. Mater.*, **327**, 126945.
<https://doi.org/10.1016/j.conbuildmat.2022.126945>

He, W. (2013), *Research For Testing The Properties Of Fresh Wet-Mix Shot Crete*, Concrete.

Hemphill, G.B. (2013), *Practical Tunnel Construction*, Jone Wiley & Sons.

Huang, S. (2006), *Application of high titanium blast furnace slag in concrete material*, New Building Materials, November.

Jiang, F., He, P., Wang, G., Zheng, C., Xiao, Z., Wu, Y. and Lv, Z. (2022), “Q-method optimization of tunnel surrounding rock classification by fuzzy reasoning model and support vector machine”, *Soft Comput.*, **26**, 1-14.
<https://doi.org/10.1007/s00500-021-06581-9>

Jin, H., Xu, H., Yang, S., Xu, Z., Li, F. and Hu, Z. (2020), “Grey target decision analysis of optimum mixing ratio of LWAS based on the comprehensive performance”, *Constr. Build. Mater.*, **262**, 120570.
<https://doi.org/10.1016/j.conbuildmat.2020.120570>

Li, Q. (2012), *Experimental Study of the Effect on the Performance of HPC with Different Mixture*, Concrete.

Li, S. (2021), “On the Construction Technology of Sprayed Concrete in Highway Tunnels”, *China Build. Mater. Technol.*, **30**(05), 154-156.

Liu, Z. (2015), *Exploration and Application of Concrete Strength*, Concrete.

Liu, F. (2019), “Experimental analysis of mechanical properties of steel fiber lightweight concrete”, Chongqing Jiaotong University, China.

Liu, X. (2020), “Experimental analysis of mechanical properties of steel fiber lightweight concrete”, Heilongjiang University, China.

Lu, L.H. (2018), “Application of Tailing Sand Steel Fiber Sprayed Concrete in Iron Mine Tunnel”, *J. Shenyang Univ. Technol.*, **1**(1). [In Chinese]

Luo, F. (2018), “Research on tailings steel fiber shotcrete in iron mine roadways”, Master Dissertation; Shenyang University of Technology, **5**(1). [In Chinese]

Mansoor, Y. and Zhang, Z. (2012), “Development of Inspection System for Crack in R.C. Tunnel Lining by Using Knowledge-Based System (KBS)”, *Adv. Mater. Res.*, **622-623**, 1415-1420.
<https://doi.org/10.4028/www.scientific.net/AMR.622-623.1415>

Mingqiang, D. (2019), “Study on the Influence of Polycarboxylate Water-Reducing Agent Content on Concrete Performance”, *Fujian Transportation Technology*.

Mou, T. (2014), *Preparation and Application of High Performance Pumping Concrete using Heavy Titanium Slag Sand*, Concrete.

- Pisova, B. and Hilar, M. (2017), "Spray-applied waterproofing membranes: effective solution for safe and durable tunnel linings?", *IOP Conference Series: Materials Science and Engineering*, Vol. 236, p. 012087.
<https://doi.org/10.1088/1757-899X/236/1/012087>
- Sakoparnig, M., Galan, I., Kusterle, W., Lindlar, B., Koraimann, G., Angerer, T., Steindl, F., Briendl, L., Jehle, S., Flotzinger, J., Juhart, J. and Mittermayr, F. (2023), "On the significance of accelerator enriched layers in wet-mix shotcrete", *Tunnell. Undergr. Space Technol.*, **131**, 104764.
<https://doi.org/10.1016/j.tust.2022.104764>
- Shaposhnik, Y. (2018), "Selecting shotcrete composition for Vostoksvetmet mines", *IOP Conference Series: Earth and Environmental Science*, Vol. 134, p. 012059.
<https://doi.org/10.1088/1755-1315/134/1/012059>
- Shuyuan, W. (2016), "Comparison between range analysis and variance analysis of concrete orthogonal test results", *Development Guide to Building Materials*.
- Sun, J., Li, R.Y.M., Jiao, T., Wang, S., Deng, C. and Zeng, L. (2023), "Research on the Development and Joint Improvement of Ceramsite Lightweight High-Titanium Heavy Slag Concrete Precast Composite Slab", *Buildings*, **13**(1), 3.
<https://doi.org/10.3390/buildings13010003>
- Thomas, A. (2009), *Sprayed Concrete Lined Tunnels*, CRC Press.
<https://doi.org/10.1201/9781482265682>
- Topçu, İ. and Bilir, T. (2010), "Experimental investigation of drying shrinkage cracking of composite mortars incorporating crushed tile fine aggregate", *Mater. Des.*, **31**, 4088-4097.
<https://doi.org/10.1016/j.matdes.2010.04.047>
- Wang, Z.Q., Shi, Y., Li, J.Z. and Yan, X.H. (2012), "Study on indoor test methods and performance of shotcrete", *J. Yangtze River Scientif. Res. Inst.*, **29**(3), 59-61.
<https://doi.org/10.3969/j.issn.1001-5485.2012.03.012>
- Xue, X., Su, Z., Sun, Z. and Song, F. (2014), "Instability Mechanism and Supporting Measure for Highway Tunnel with High Ground Stress and Soft Surrounding Rock", *Advanced Materials Research*, 1049-1050, 213-216.
<https://doi.org/10.4028/www.scientific.net/AMR.1049-1050.213>
- Yan, R. (2021), "Experimental Study on Preparation and Working Mechanical Properties of Steel Fiber Reinforced Concrete", *Jiangxi Building Materials*.
- Yan, S., Jiao, H., Yang, X., Wang, J. and Chen, F. (2020), "Bending Properties of Short-Cut Basalt Fiber Shotcrete in Deep Soft Rock Roadway", *Adv. Civil Eng.*, **2020**, 1-9.
<https://doi.org/10.1155/2020/5749685>
- Yang, F. (2015), "Research on Application of High Strength Shotcrete in Railway Tunnels", *Railway Engineering*.
- Yu, L. (2005), "Numerical analysis on tunnel excavation and support in soft rock", Dalian University of Technology, China.
- Zhang, T. and Pan, D. (2021), "Mechanical properties of steel-polypropylene hybrid fiber reinforced concrete in building structure: steel-polypropylene hybrid fiber reinforced concrete in building structure", *Stavební obzor - Civil Eng. J.*, **30**.
<https://doi.org/10.14311/CEJ.2021.02.0037>
- Zhen, H., Zhang, C., Ma, S., Chen, Y. and Liao, M. (2021), "Design and key technology analysis of integrated robot system for tunnel maintenance", *J. Rail Way Sci. Eng.*, **18**(3), 767-776.
<https://doi.org/10.19713/j.cnki.43-1423/u.T20200506>
- Zhu, Y. (2009), "Study on mechanical properties of steel fiber shotcrete and its application in tunnel single-layer lining", Chongqing University, China.